

## **Low-temperature, green synthesis of multivalent manganese oxide nanowires**

Harish Veeramani<sup>1, 4</sup>, Deborah Aruguete<sup>2</sup>, Niven Monsegue<sup>3</sup>, Mitsuhiro Murayama<sup>3, 4</sup>, Urs Dippon<sup>5</sup>,  
Andreas Kappler<sup>5</sup>, and Michael F. Hochella Jr.<sup>1,4</sup>

<sup>1</sup>Center for NanoBioEarth, Department of Geosciences, Virginia Tech, Blacksburg, VA 24061, USA

<sup>2</sup> Division of Earth Sciences, National Science Foundation, Arlington, Virginia 22230, USA

<sup>3</sup> Department of Materials Science and Engineering, Virginia Tech, Blacksburg, VA 24061, USA

<sup>4</sup> Institute for Critical Technology and Applied Science, Virginia Tech, Blacksburg, VA 24061, USA

<sup>5</sup> Geomicrobiology, Center for Applied Geoscience, Eberhard-Karls-University Tuebingen, 72076  
Tuebingen, Germany

### **Supplementary Information**

#### **1. *Mn(II) analysis***

Samples were withdrawn at various time intervals and acidified in MES (2-(N-morpholino)ethanesulfonic acid) buffer (pH 5.5) to arrest further Mn(II) oxidation. The samples were then centrifuged (120000 X g) for 5 minutes and the supernatant was filtered through a 0.2 µm polyethersulfone syringe filter (VWR 28145-499) and refrigerated (4°C) until analysis. The filtered samples were diluted 200 times in ultrapure MilliQ water and analyzed for its Mn(II) content using the formaldoxime spectrophotometric method (Morgan and Stumm, 1965; Brewer and Spencer, 1971). Briefly, the formaldoxime stock reagent was prepared by mixing a solution of 10% hydroxylamine hydrochloride with 37% formaldehyde solution (2:1 ratio). 4 mL of the formaldoxime reagent was further mixed with 2 mL of concentrated ammonium hydroxide solution (28 – 30%) and used for the analysis. Briefly, 0.875 mL of the diluted sample was mixed with 0.125 mL of the formaldoxime reagent within semi-micro disposable plastic cuvettes (VWR

97000-590) to yield a reddish-brown color. The absorbance of the reaction mixture and Mn(II) standards were measured at 450 nanometers in a Beckman DU 640 spectrophotometer.

## **2. Powder X-ray diffraction (XRD)**

Powder X-ray diffraction (XRD) was performed to identify the mineral phases in synthesized products. Diffraction measurements were carried out using a Rigaku MiniFlex benchtop X-ray diffractometer (Rigaku, The Woodlands, TX) equipped with a Cu source ( $\text{CuK}\alpha_1$ ,  $\lambda=1.5406 \text{ \AA}$ ). The suspension of hematite (before and after Mn(II) oxidation) was centrifuged at 10000xg for 10 minutes and the supernatant was discarded. The pellet was applied as a paste to zero-background silicon sample holder and allowed to air-dry. Diffraction measurements were carried out with a start and end angle of  $10^\circ/2\theta$  and  $90^\circ/2\theta$  respectively, step width of  $0.05^\circ(2\theta)$  and a scan speed of  $2.00^\circ/\text{min}(2\theta)$ . The X-ray tube voltage was set at 30 kV and the tube current at 15 mA.

## **3. Atomic Force Microscopy (AFM)**

The suspension of iron oxide after complete Mn(II) oxidation was centrifuged at 10000xg for 10 minutes and the supernatant was discarded. The pellet was suspended in few drops of ultrapure water and the suspension was applied as a thin film to a round glass coverslip (Ted Pella) and allowed to air-dry. Excess water was removed from the surface gently using a Kimwipe tissue. The glass coverslip containing the sample was analyzed by a Veeco MultiMode Atomic Force Microscope (Veeco Metrology, Santa Barbara, CA). The AFM was operated in tapping mode using an antimony (n) doped Si tapping mode probe (Veeco Instruments, Bruker Corporation, USA). The cantilever had a spring constant of  $20\text{--}80 \text{ N m}^{-1}$ , resonant frequency of 230-410 kHz, length of 110-140  $\mu\text{m}$  and thickness of 3.5-4.5  $\mu\text{m}$  and width of 25-35  $\mu\text{m}$ . The nominal tip radius of the probe was 8 nm and the maximum tip radius was 12 nm. The AFM scan rate was 0.5 Hz with a scan size of 500 and 512 grid points per scan line. Analysis of the AFM images was done using Digital Instruments, NanoScope IIIa software (version 5.30r3sr3).

#### **4. Mössbauer Spectroscopy**

Samples for Mössbauer were prepared by filtering the mineral suspensions through 0.45 µm pore-size filters (MF-Millipore Membrane, mixed cellulose esters, Hydrophilic, 13 mm). Filters containing the retained solids were sealed using Kapton tape and analyzed using a spectrometer (Wissenschaftliche Elektronik GmbH, Germany). Samples were mounted in a closed-cycle helium cryostat (Janis Research Company, Inc., USA) that allowed cooling of the sample to 5.5 K. Mossbauer spectra were collected in transmission mode using a <sup>57</sup>Co source embedded within a Rhodium matrix. The source was operated at room temperature using a constant acceleration drive system set to a velocity range of ±12 mm/s with movement error of <1%. The absorption was recorded using a proportional counter and a 1024-multichannel analyzer. The spectra were calibrated against a room temperature spectrum of alpha-Fe metal foil. Folding and fitting of the spectra was performed using the Recoil software suite (University of Ottawa, Canada).

#### **5. Sample Preparation for Electron Microscopy**

At various sampling times, an additional 0.1 mL of the suspension was withdrawn and centrifuged at 10000 x g for 5 minutes. The supernatant was discarded and the pellet was resuspended in 2 mL of ultrapure water. This procedure was repeated five times and the final suspension was diluted 10 times using ultrapure water. Samples for electron microscopic and analytical characterization were prepared by depositing this diluted mixture onto double-layer carbon-coated copper grids (Pacific Grid-Tech Cu-300HD) and allowed them to air-dry. Subsequently, the TEM grids containing the samples were washed gently using ultrapure water.

For cross-sectional imaging, an aliquot of the undiluted suspension was embedded in epoxy resin (Poly/Bed® 812) and microtomed using a diamond knife (Leica Ultracut UCT, Australia). Sections approximately 60–90 nm thick were collected on 200-mesh, formvar-coated Cu grids (Ted Pella) for TEM analysis.

## 6. Figures

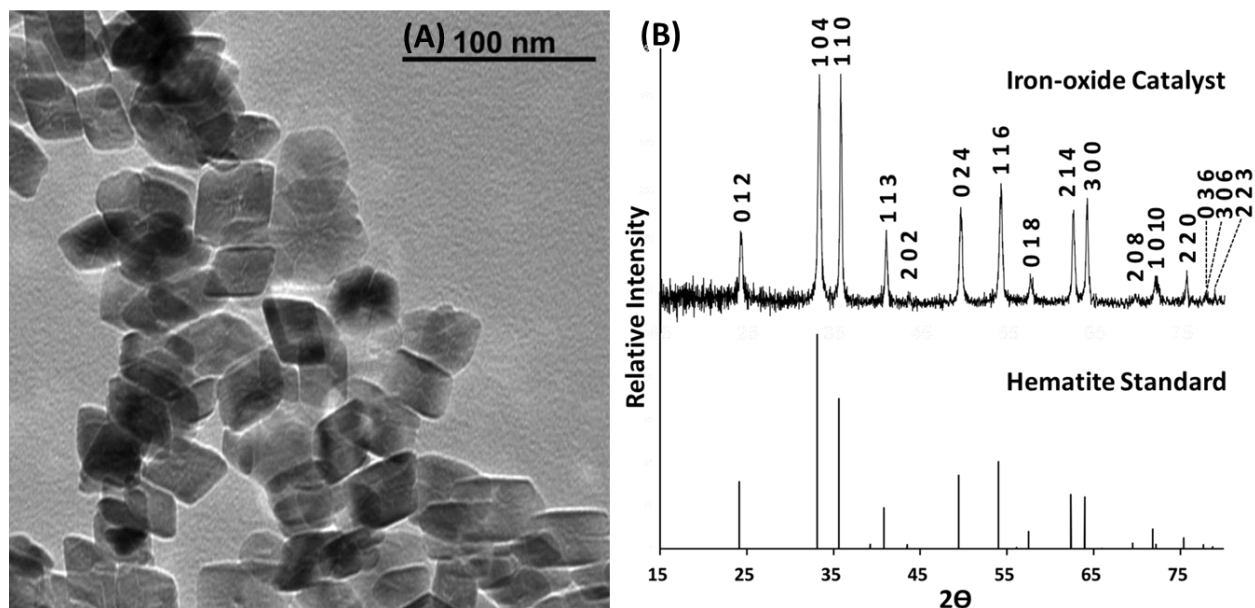


Figure S1: (A) TEM image and (B) Powder X-ray Diffraction patterns of rhombohedral iron-oxide catalyst nanoparticles used in the present study. Absence of other peaks in the XRD spectrum is indicative of a pure hematite phase. The spectrum on top of the stack plot corresponds to the iron-oxide catalyst sample and the reference spectrum (ICDD database - PDF Card # 01-072-0469) on the bottom is included for comparison.

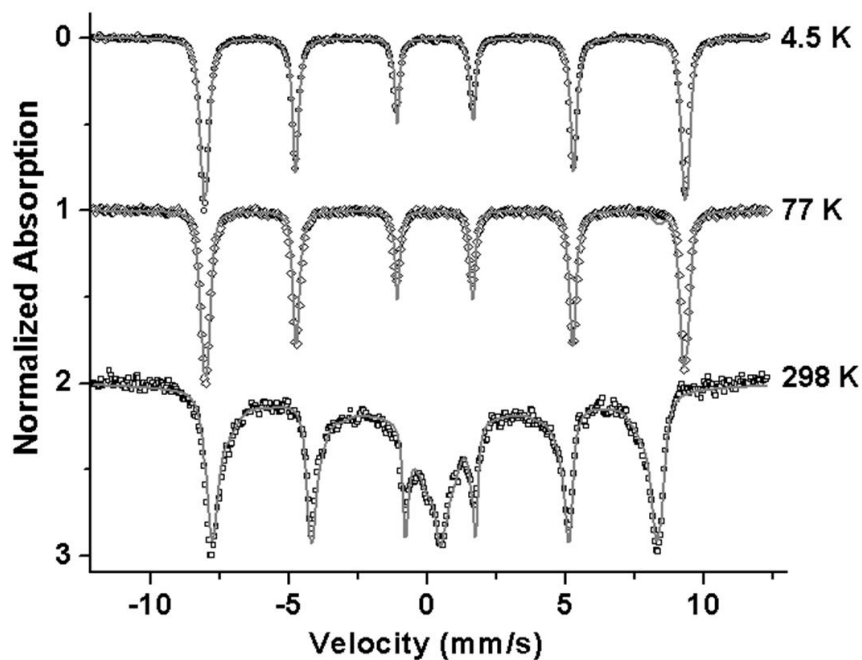


Figure S2: Mössbauer spectra at various temperatures of the iron-oxide catalyst nanoparticles that was used prior to  $\text{Mn}_3\text{O}_4$  nanowire synthesis. The measurements are indicated in circles and the model used to fit data is depicted as a solid line. Mössbauer analyses indicate the iron-oxide catalyst to be pure hematite. The Mössbauer spectra look identical after Mn(II) oxidation suggesting no phase transformation with respect to the iron-oxide (data not shown)

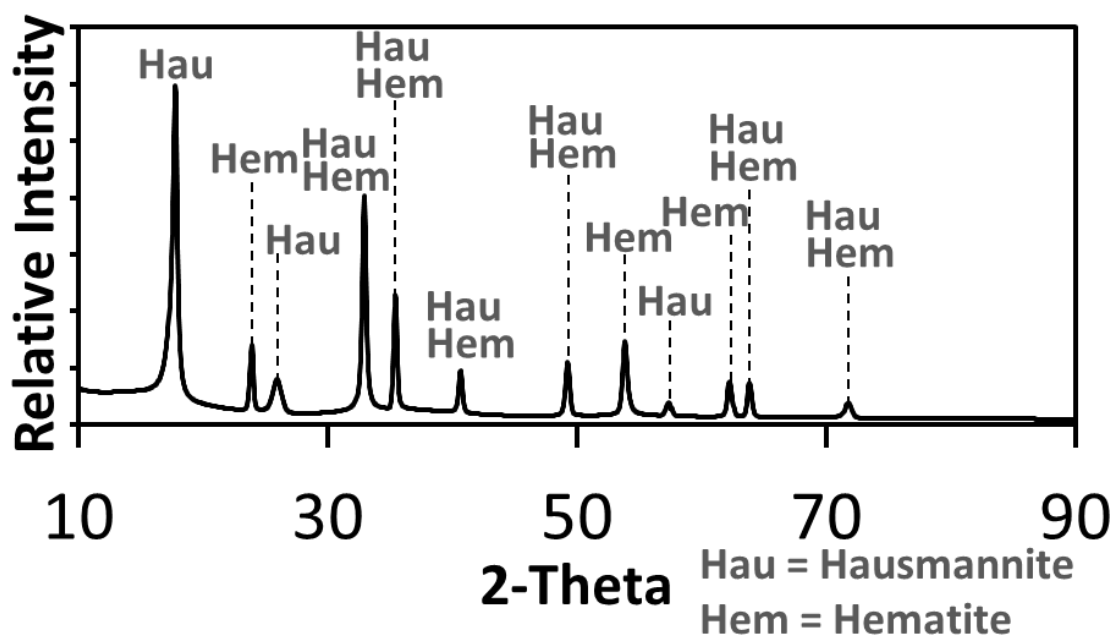


Figure S3: Powder XRD diffractogram of the iron-oxide catalyst nanoparticles and the  $Mn_3O_4$  product. The XRD diffractogram of the Hausmannite sample was compared to the PDF Card # 03-065-1123 from the ICDD Database.

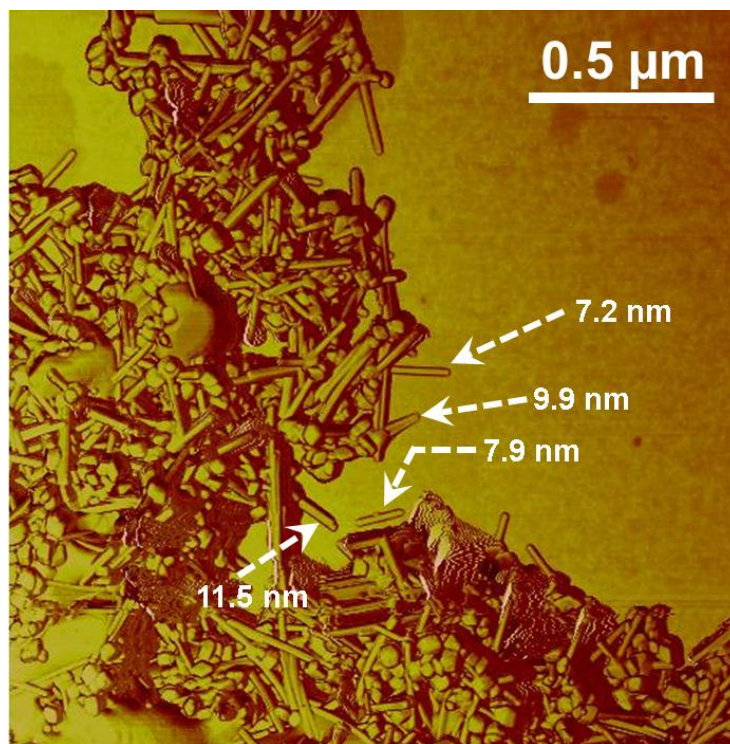


Figure S4: Atomic Force Microscopy (AFM) images of the  $Mn_3O_4$  nanowires. The values indicated are vertical distances recorded by the instrument.

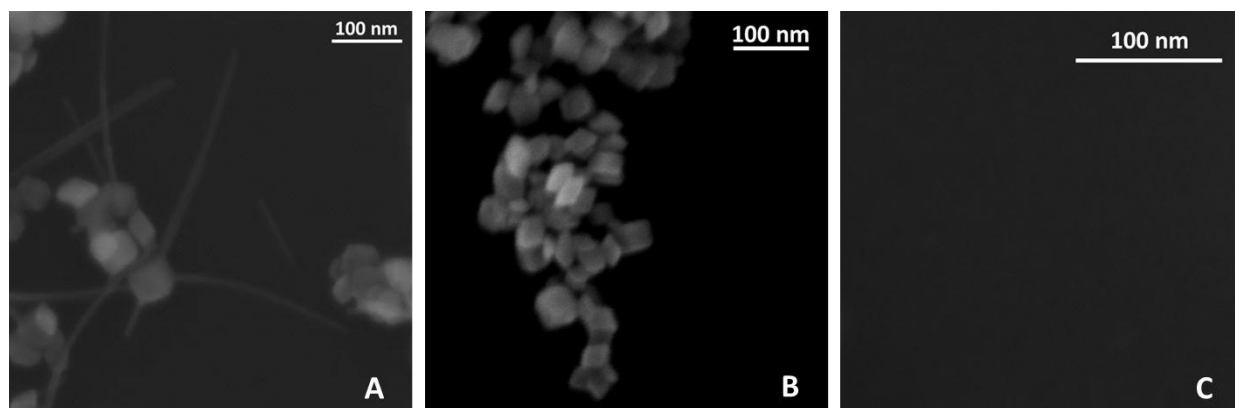


Figure S5: SEM images of (A)  $\text{Mn}_3\text{O}_4$  nanowires in presence of the nano iron-oxide catalyst, (B) nano iron-oxide catalyst in the absence of  $\text{Mn}^{2+}$  and (C) absence of iron-oxide